

C–H Bond Activation in Aqueous Solution: Kinetics and Mechanism of H/D Exchange in Alcohols Catalyzed by Molybdocenes

Christoph Balzarek, Timothy J. R. Weakley, and David R. Tyler*

Contribution from the Department of Chemistry, University of Oregon, Eugene, Oregon 97403

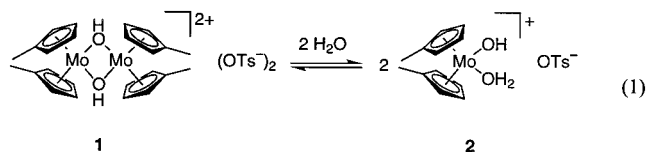
Received May 3, 2000

Abstract: The mechanism of the catalytic H/D exchange in alcohol substrates promoted by molybdocenes in D₂O was shown to occur by C–H bond activation. Primary alcohols selectively exchanged α -hydrogens in aqueous solutions containing the catalyst precursor [Cp'₂Mo(μ -OH)₂MoCp'₂](OTs)₂, while some additional β -hydrogen exchange was observed in secondary alcohols. Tertiary alcohols did not undergo H/D exchange. Formation of chelate complexes such as the independently synthesized and crystallographically characterized glycolate complex [Cp'₂MoOCH₂CH₂OH](OTs) inhibited the H/D exchange in multidentate alcohols. The exchange reaction was shown to proceed by formation of ketone hydride molybdocene intermediate [Cp'₂Mo(OCR¹R²)H]⁺, which can reversibly dissociate the ketone ligand. The molybdocene hydride complex resulting from ketone dissociation was identified by independent synthesis and crystallographic characterization of the hydride complex Cp'₂MoH(OTf). The H/D exchange reaction proceeds stepwise, with the active catalyst being derived from the monomeric complex [Cp'₂Mo(OH)(OH₂)]⁺. At *T* = 90 °C, the exchange of the first methylene hydrogen of PhCH₂OH occurs with a rate constant *k* = 1.16 × 10⁻⁴ (±9.88 × 10⁻⁷) s⁻¹. The activation parameters were determined as $\Delta H^\ddagger = 19.4 (\pm 0.2) \text{ kcal mol}^{-1}$ and $\Delta S^\ddagger = -22.7 (\pm 0.7) \text{ cal mol}^{-1} \text{ K}^{-1}$. A primary kinetic isotope effect of $k_{\text{H,pD6.4}}/k_{\text{D,pH6.5}} = 2.2$ was found.

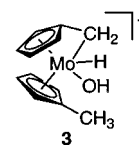
Introduction

Bent metallocenes of the type Cp₂MX₂ are soluble in aqueous solution, and over the past 15 years, the aqueous chemistry of metallocenes containing Ti,^{1,2} Zr,¹ Hf,³ V,¹ Nb,⁴ Cr,⁵ and Mo^{6,7} has been explored. These studies have shown that molybdocenes are the most stable metallocenes in water with respect to hydrolysis of the cyclopentadienyl ligands.⁶ If oxygen is excluded, no hydrolysis can be detected for aqueous solutions of molybdocenes over a period of several weeks. This remarkable stability allowed investigation of the molybdocenes' catalytic chemistry in water. Intending to gain an understanding of the origin of its antitumor activity, Kuo et al. found that aqueous solutions of Cp₂MoCl₂ are able to promote the hydrolysis of activated⁸ and unactivated⁹ phosphate esters.

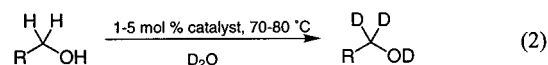
As part of our research program^{10–16} on organometallic catalysis in water,¹⁷ we investigated the aqueous chemistry of the dimeric molybdocene complex [Cp'₂Mo(μ -OH)₂MoCp'₂](OTs)₂ (**1**).^{18,19} It was shown that the chemistry of this complex in water is related to that of the molybdocene dihalides. Aqueous solutions of either **1** or Cp'₂MoCl₂ consist of the same species, where the identity of the complexes in solution depends only on the pH. Under neutral conditions, aqueous solutions contain the dimeric complex **1** in equilibrium with the monomeric aquo hydroxy complex **2** (eq 1).



When a solution of **1** was heated in D₂O, the CpCH₃ protons of the cyclopentadienyl ligands of **1** and **2** were exchanged for deuterium.¹⁹ This observation was explained in terms of an intramolecular C–H bond activation reaction proceeding through an intermediate hydride complex (**3**), analogous to the tucked-in tungstenocene complex (η^5 -Cp*)(η^5 , η^1 -C₅Me₄CH₂)WH described previously.^{16,20}



Of more interest, aqueous solutions of **1** also catalyze the intermolecular H/D exchange of α -protons in alcohols (eq 2).



Similar to the intramolecular case, a mechanism was proposed

(10) Avey, A.; Tenhaeff, S. C.; Weakley, T. J. R.; Tyler, D. R. *Organometallics* **1991**, *10*, 3607–3613.

(11) Avey, A.; Tyler, D. R. *Organometallics* **1992**, *11*, 3856–3863.

(12) Tyler, D. R. *Organometallic Radical Chemistry in Aqueous Solution. In Aqueous Organometallic Chemistry and Catalysis*; Kluwer Academic Publishers: Dordrecht, 1995; pp 47–60.

(13) Baxley, G. T.; Miller, W. K.; Lyon, D. K.; Miller, B. E.; Nieckarz, G. F.; Weakley, T. J. R.; Tyler, D. R. *Inorg. Chem.* **1996**, *35*, 6688–6693.

(14) Nieckarz, G. F.; Weakley, T. J. R.; Miller, W. K.; Miller, B. E.; Lyon, D. K.; Tyler, D. R. *Inorg. Chem.* **1996**, *35*, 1721–1724.

(15) Baxley, G. T.; Weakley, T. J. R.; Miller, W. K.; Lyon, D. K.; Tyler, D. R. *J. Mol. Catal. A: Chem.* **1997**, *116*, 191–198.

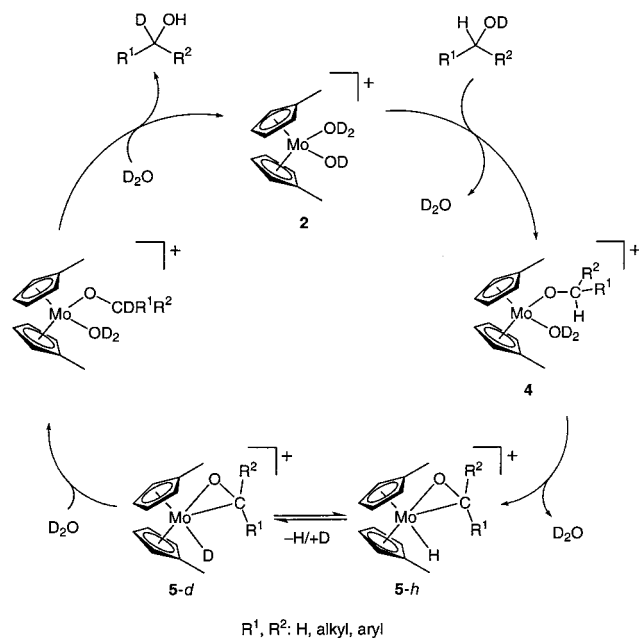
(1) Toney, J. H.; Marks, T. J. *J. Am. Chem. Soc.* **1985**, *107*, 947–953.
(2) Mokdsi, G.; Harding, M. M. *J. Organomet. Chem.* **1998**, *565*, 29–35.

(3) Murray, J. H.; Harding, M. M. *J. Med. Chem.* **1994**, *37*, 1936–1941.
(4) Harding, M. M.; Prodigalidad, M.; Lynch, M. J. *J. Med. Chem.* **1996**, *39*, 5012–5016.

(5) Spreer, L. O.; Shah, I. *Inorg. Chem.* **1981**, *20*, 4025–4027.
(6) Kuo, L. Y.; Kanatzidis, M. G.; Marks, T. J. *J. Am. Chem. Soc.* **1987**, *109*, 7207–7209.

(7) Kuo, L. Y.; Kanatzidis, M. G.; Sabat, M.; Tipton, A. L.; Marks, T. J. *J. Am. Chem. Soc.* **1991**, *113*, 9027–9045.

(8) Kuo, L. Y.; Kuhn, S.; Ly, D. *Inorg. Chem.* **1995**, *34*, 5341–5345.
(9) Kuo, L. Y.; Barnes, L. A. *Inorg. Chem.* **1999**, *38*, 814–817.

Scheme 1. Postulated Mechanism for H/D Exchange in Alcohols

that involves the activation of the C–H bond of the alcohol after coordination of the substrate to the metal center (Scheme 1). The most notable step in this mechanism is the insertion of the metal center into the C–H bond of the alcohol (**4** to **5-h**). The activation of a C–H bond in aqueous medium is strongly sought after,²¹ yet only a few examples of this reaction type are known that occur in water²² and that are catalytic in the metal complex employed.^{23,24}

In this paper we present experimental evidence in support of the proposed mechanism for H/D exchange in alcohols. This includes the isolation and characterization of important intermediates and analysis of the reaction kinetics. Additionally, the implications of this mechanism for the use of the molybdocene catalyst in other reactions is discussed.

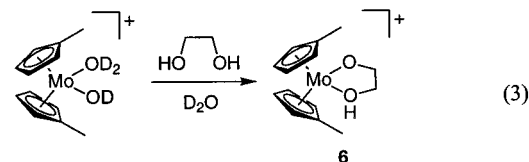
Results and Discussion

Deuterium Exchange in Alcohols. After the initial observation of H/D exchange in methanol (eq 2, $R = \text{H}$),¹⁹ a number of alcohols and other substrates were tested in this reaction. A solution of the substrate and catalyst **1** in D_2O in a sealed NMR tube was heated for several hours, and the disappearance of the $\alpha\text{-H}$ signals in the ^1H NMR were monitored periodically. In addition, ^2H NMR spectra were recorded to confirm the presence of the deuterated product. The results of these experiments are shown in Table 1. Primary alcohols are selectively converted into the α,α -deuterated products, while secondary alcohols show

Table 1. Intermolecular H/D Exchange with Alcoholic Substrates

substrate	$c(\text{ROH})$ (M)	mol % of cat. (1)	T ($^\circ\text{C}$)	t (h)	% H/D exchange
MeOH	1.02	0.9	102	39:00	67
EtOH	0.71	2.6	102	39:00	30
ⁿ PrOH	0.55	3.2	85	68:40	48
ⁿ BuOH	0.45	3.7	85	22:00	33
benzyl alcohol	0.28	4.8	80	21:30	90
	0.19	7.8	80	46:00	>99
2-propanol	0.36	4.3	86	20:40	23
2-butanol	0.25	4.8	80	34:00	14
<i>tert</i> -butyl alcohol	0.29	5.0	80	5 days	0
ethylene glycol	0.38	3.6	88	29:30	6
1,3-propanediol	0.40	6.5	80	10 days	39

incorporation of D on both α - and β -carbons. No H/D exchange is observed in *tert*-butyl alcohol. The lack of reactivity in the latter alcohol, which does not possess α -hydrogens, is readily explained by the proposed mechanism which proceeds by insertion of the metal center into the $\alpha\text{-C-H}$ bond (Scheme 1, **4** \rightarrow **5-h**). With bidentate alcohols such as ethylene glycol, the reaction slows down significantly and a third major molybdocene species in addition to **1** and **2** is observed in the reaction solution by ^1H NMR ($\delta = 5.38$ (m), 5.33 (m), 3.24 (s), 1.83 (s) ppm). The integral ratio and chemical shifts of the observed resonances are consistent with a 1:1 molybdocene ethylene glycol adduct **6** (eq 3; this product is discussed further below).



The reactions of ketones under H/D exchange conditions result in β -deuteration. This is assumed to occur by simple protonation/deprotonation facilitated by coordination of the substrate to the molybdocene, which results in a decreased $\text{p}K_a$ for the ketone. Other nonalcoholic substrates such as ethers (THF , Et_2O) or amines (HNEt_2 , NEt_3 ; buffered in neutral aqueous solution) did not undergo H/D exchange.

Preparation and Structure of the Molybdocene Glycolate (6**).** Glycolate complex **6** was prepared independently in order to confirm the identity of the unknown molybdocene species formed from ethylene glycol under H/D exchange conditions. The glycolate could be isolated from an alcohol solution of **1** and ethylene glycol. The ^1H NMR spectrum of **6** showed resonances identical to those found in the H/D exchange reaction solution ($\delta = 5.38$ (m), 5.33 (m), 3.24 (s), 1.83 (s) ppm).

Orange crystals of **6** suitable for X-ray diffraction were grown from methanol. The asymmetric unit contains two cations of very similar structure and two tosylate anions. The 1:1 stoichiometry implies that the glycolate ligand is monoprotonated. The quality of the data set did not allow the direct location of the protonation sites. However, in each cation there is one short and one longer Mo–O bond, 2.013(4) Å and 2.151(4) Å, respectively, for the fragment shown in Figure 1. Each of the oxygens that forms the longer bonds also makes a short contact with a sulfonate oxygen of a tosylate anion (see Supporting Information), implying that it is a proton donor.

A few neutral molybdocene alkoxide complexes from chelating diols have previously been prepared and characterized spectroscopically,^{25,26} but only one complex, $\text{Cp}_2\text{Mo}(\text{OCH}(\text{CF}_3)_2)_2$, has been characterized crystallographically.²⁷ In this

(25) Green, M. L. H.; Lindsell, W. E. *J. Chem. Soc. A* **1967**, 1455–1458.

(16) Yoon, M.; Tyler, D. R. *Chem. Commun.* **1997**, 639–640.

(17) For reviews see: (a) Horváth, I.; Joó, F. *Aqueous Organometallic Chemistry and Catalysis*; Kluwer Academic Press: Dordrecht, 1995. (b) Cornils, B.; Herrmann, W. A. *Aqueous Phase Organometallic Catalysis*; Wiley-VCH: Weinheim, 1998. (c) Herrmann, W. A.; Kohlpaintner, C. W. *Angew. Chem.* **1993**, 32, 1524–1544.

(18) Balzarek, C.; Weakley, T. J. R.; Kuo, L. Y.; Tyler, D. R. *Organometallics* **2000**, 19, 2927–2931.

(19) Balzarek, C.; Tyler, D. R. *Angew. Chem., Int. Ed.* **1999**, 38, 2406–2408.

(20) Parkin, G.; Bercaw, J. E. *Organometallics* **1989**, 8, 1172–1179.

(21) Arndtsen, B. A.; Bergman, R. G.; Mobley, T. A.; Peterson, T. H. *Acc. Chem. Res.* **1995**, 28, 154–162.

(22) Shilov, A. E.; Shul'pin, G. B. *Chem. Rev.* **1997**, 97, 2879–2932.

(23) Regen, S. L. *J. Org. Chem.* **1974**, 39, 260–261.

(24) Stahl, S. S.; Labinger, J. A.; Bercaw, J. E. *J. Am. Chem. Soc.* **1996**, 118, 5961–5976.

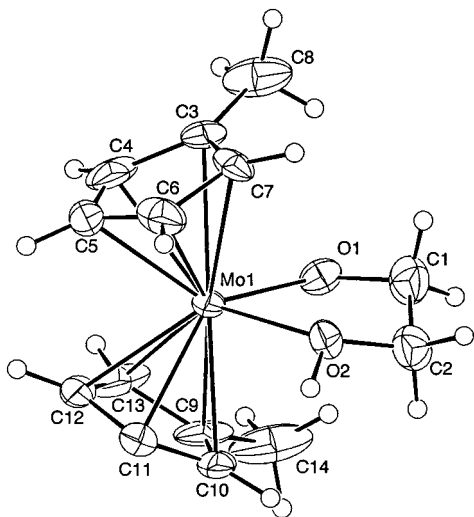
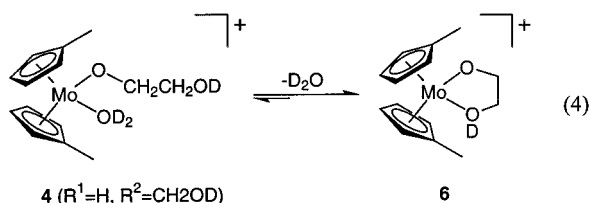


Figure 1. Molecular structure of $[\text{Cp}'_2\text{Mo}(\text{OCH}_2\text{CH}_2\text{OH})]^+$ (**6**). Only one cation is shown. Selected bond lengths (Å): Mo(1)–O(1), 2.013(4); Mo(1)–O(2), 2.151(4).

latter compound, the Mo–O bond lengths were determined as 2.065(5) Å and 2.101(5) Å, comparable to the bond lengths found in **6**.

Mechanistic Implications of Glycolate Formation. Two significant arguments for the proposed mechanism can be made on the basis of the reactivity of ethylene glycol under H/D exchange conditions. First, because the exchange reaction is significantly slower than for monodentate alcohols, this argues against a simple protonation/deprotonation mechanism, facilitated by the molybdenum complex. If coordination of the alcohol resulted in a decreased $\text{p}K_a$ of the alcohol α -hydrogens, thereby making simple proton exchange more facile, the rate of the exchange reaction in aliphatic monodentate alcohols and ethylene glycol should not show any significant difference. Second, inhibition by a chelating alcohol shows that not only is coordination of the substrate required in the reaction sequence but an additional vacant coordination site has to become available. The required coordination site is occupied in the complex formed in the reaction of the molybdocene fragment and ethylene glycol (eq 4). It is the chelating ability of ethylene



glycol that explains the sluggishness of the H/D exchange with this substrate. Also note that complex **6** is obtained as the monocation, with one glycol oxygen remaining protonated in the solid state. This is consistent with the proposed monocationic molybdocene intermediates along the reaction pathway.

Observation of Free Ketone and Preparation of the Hydride Intermediate. In the reaction solution of 2-propanol under standard H/D exchange conditions, a small amount of acetone, which is slowly deuterated, was detected by ^1H NMR spectroscopy. In addition to free acetone, a set of four resonances with signals in the Cp region ($\delta = 4.87, 4.66, 4.08,$ and 3.57 ppm) were observed.

(26) Ribeiro da Silva, M. A. V.; Ribeiro da Silva, M. M. C.; Dias, A. R. *J. Organomet. Chem.* **1988**, *345*, 105–115.

(27) Hunger, M.; Limberg, C.; Kircher, P. *Angew. Chem., Int. Ed.* **1999**, *38*, 1105–1108.

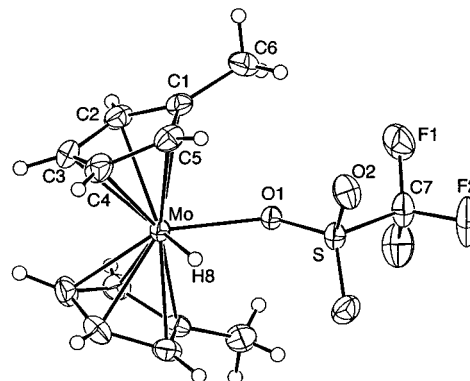
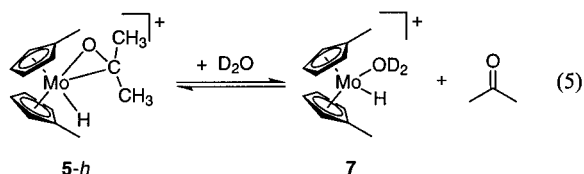
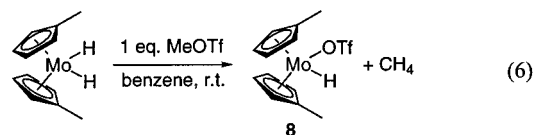


Figure 2. Molecular structure of $\text{Cp}'_2\text{MoH}(\text{OTf})$ (**8**). Selected bond lengths (Å): Mo–H(8), 1.53(3); Mo–O(1), 2.186(2).

ppm) of the ^1H NMR spectrum were observed. These resonances are common for all H/D exchange reactions, independent of the nature of the alcohol substrate. Free acetone could conceivably arise from dissociation of the π -bonded ketone ligand from intermediate **5**. This would result in a molybdocene monohydride complex (**7**, eq 5).



To verify this assumption, the monohydride complex $\text{Cp}'_2\text{MoH}(\text{OTf})$ (**8**) was prepared. The synthesis of **8** (eq 6) was carried out similarly to the preparation of the cationic $[\text{Cp}'_2\text{WH}(\text{C}_4\text{H}_8\text{O})][\text{CF}_3\text{SO}_3]$.²⁸ Thus, treatment of $\text{Cp}'_2\text{MoH}_2$ with 1 equiv of $\text{MeOSO}_2\text{CF}_3$ in benzene at room temperature resulted in the formation of solvent-free monohydride **8**.



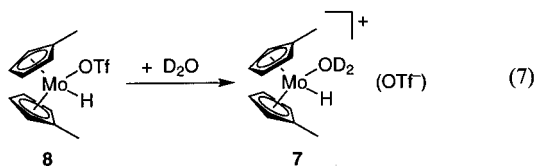
Orange-red crystals grown from hot benzene were analyzed by X-ray crystallography (Figure 2). Unlike the tungsten analogue, which was prepared in coordinating solvents,²⁸ the molybdocene hydride was isolated as the neutral complex with the triflate anion occupying one of the equatorial coordination sites. The Mo–H bond length of 1.53(3) Å is short for a molybdocene hydride complex,²⁹ but not unusual, as the Mo–H bond distance in the fumaronitrile complex $\text{Cp}_2\text{Mo}(\text{H})\text{-(CHCNCH}_2\text{CN)}$ was found to be 1.529 Å.³⁰

Hydride complex **8** dissolved slowly in water to give a faint yellow solution (eq 7). In D_2O , four Cp resonances were observed at $\delta = 4.87, 4.66, 4.08,$ and 3.57 ppm, corresponding to those found in the H/D exchange reaction solution for the species suggested to be **7**. This reaction confirms the assignment

(28) Carmichael, A. J.; McCamley, A. *J. Chem. Soc., Dalton Trans.* **1997**, 93–98.

(29) The bond length for Cp_2MoH_2 was determined by neutron diffraction as 1.685(3) Å: (a) Schultz, A. J.; Stearley, K. L.; Williams, J. M.; Mink, R.; Stucky, G. D. *Inorg. Chem.* **1977**, *16*, 3303–3306. Other Mo–H bond lengths were found to be of the order of 1.7 Å: (b) Azevedo, C. G.; Calhorda, M. J.; Carrondo, M. A. A. F. d. C. T.; Dias, A. R.; Felix, V.; Romao, C. C. *J. Organomet. Chem.* **1990**, *391*, 345–360. (c) Koloski, T. S.; Pestana, D. C.; Carroll, P. J.; Berry, D. H. *Organometallics* **1994**, *13*, 489–499.

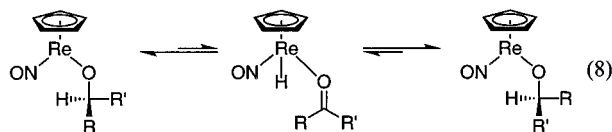
(30) Ko, J. J.; Bockman, T. M.; Kochi, J. K. *Organometallics* **1990**, *9*, 1833–1842.



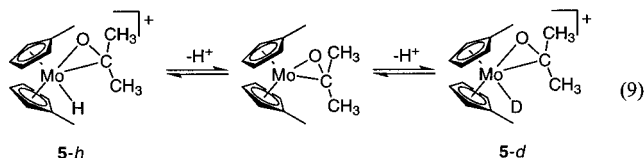
of the common metallocene intermediate in the H/D exchange reactions as the molybdocene monohydride (eq 5). Characteristic of the metal hydride is the resonance observed at $\delta = -8.41$ ppm. This resonance decreases over several days at room temperature in D_2O . For the Cp analogue, the exchange of the hydride ligand by a deuteride was confirmed by 2H NMR.³¹

Comments on the Proposed Ketone Hydride Intermediate (5). The formation of π -ketone intermediate **5** (Scheme 1) is not unreasonable³² because ketone complexes of molybdocenes have previously been prepared.^{33–35} In addition, the structure of the formaldehyde complex $Cp_2Mo(\eta^2-OCH_2)$ was determined, showing side-on π -coordination of the carbonyl moiety.³³ This thermally robust complex readily underwent protonolysis with trifluoroacetic acid to yield $Cp_2Mo(O_2CCF_3)_2$ and MeOH.³⁶ This result is consistent with the mechanism in Scheme 1, whose main features are reversible π -ketone complex formation (**5**) and subsequent alcohol elimination.

The reversible β -H activation in alcohols has been described previously by Saura-Llamas and Gladysz.³⁷ They showed that chiral alcohols racemized rapidly in benzene solution in the presence of $CpRe(PPh_3)(NO)(OMe)$. This process was proposed to proceed through a ketone complex intermediate in which the chiral alcohol replaced the OMe ligand (eq 8). No free ketone was observed, which was taken as an indicator that the racemization process proceeded intramolecularly.



Precedents also exist for the reversible deprotonation/protonation of molybdocene complexes with π -coordinated ligands. Such reactions have been observed by Benfield and Green,³⁸ who reported that the cationic complex $[Cp_2MoLH][PF_6]$ (L = ethylene, propylene) can be converted to the olefin complex Cp_2MoL by treating it with dilute aqueous base. Addition of aqueous NH_4PF_6 to the neutral olefin complex converted it back to the parent molybdocene hydride olefin complex. These results suggest that the exchange of the hydride ligand by a deuteride likely occurs by a dissociative pathway (eq 9).³⁹



(31) L. Y. Kuo, personal communication.

(32) It is important to note that a σ -bonded ketone complex could be considered as an alternative formulation of the ketone hydride complex **4**. Trispyrazolylborate complexes of Mo and W have recently been shown to contain σ - or π -bonded ketones, depending on steric strain: Schuster, D. M.; White, P. S.; Templeton, J. L. *Organometallics* **2000**, *19*, 1540–1548.

(33) Gambarotti, S.; Floriani, C.; Chiesi-Villa, A.; Guatini, C. *J. Am. Chem. Soc.* **1985**, *107*, 2985–2986.

(34) Herberich, G. E.; Okuda, J. *Angew. Chem., Int. Ed. Engl.* **1985**, *24*, 402.

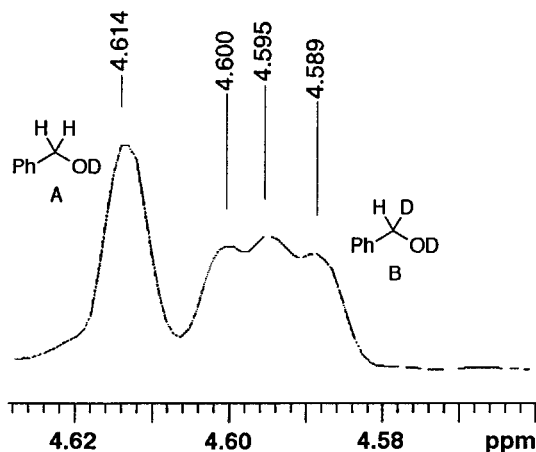
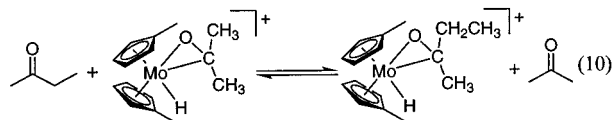


Figure 3. 1H NMR spectrum of $PhCH_2OD$ (**A**) and $PhCHDOD$ (**B**) in D_2O .

Transfer Hydrogenation. To elucidate whether the ketone dissociation is reversible, the H/D exchange reaction with 2-propanol as the substrate was carried out in the presence of an equal amount of 2-butanone. After 21 h at 80 °C, the reaction mixture contained 2-butanol and acetone in addition to the starting materials, 2-propanol and 2-butanone. This indicates an equilibrium for ketone dissociation that can be described as shown in eq 10.



The overall result of this reaction is the conversion of a ketone into an alcohol, using a sacrificial alcohol as hydrogen donor, resembling the Meerwein–Ponndorf–Verley reduction. Transfer hydrogenations of this type are well documented for late transition metals in *organic* solvents.^{40–42} The molybdocene-promoted reaction, however, is carried out in *water* with an early-transition-metal catalyst.

Stepwise Exchange. The disappearance of the methylene resonance of benzyl alcohol at 90 °C in D_2O was followed by 1H NMR (Figure 3). The integral over the methylene region of benzyl alcohol relative to the integral of the aromatic region for the benzyl alcohol was used to calculate the total concentration of methylene protons present in solution. This integral includes proton resonances from $PhCH_2OD$ (**A**), contributing two protons per **A**, and from the monodeuterated product, $PhCHDOD$ (**B**), contributing one proton per **B**. The total concentration of protons can therefore be expressed as $[protons] = 2[A] + [B]$ (Figure 4, squares). Because of a small isotope shift of the **B** methylene resonance (Figure 3), the concentrations

(35) Okuda, J.; Herberich, G. E. *Organometallics* **1987**, *6*, 2331–2336.

(36) See footnote 28 in ref 35.

(37) Saura-Llamas, I.; Gladysz, J. A. *J. Am. Chem. Soc.* **1992**, *114*, 2136–2144.

(38) Benfield, F. W. S.; Green, M. L. H. *J. Chem. Soc., Dalton Trans.* **1974**, 1324–1331.

(39) Although precedents exist for the dissociative H^+/D^+ exchange (eq 9),³⁸ alternative pathways cannot completely be ruled out. These pathways include an associative process involving the formation of a $[Cp_2Mo(\pi-ketone)(H)(D)]^{2+}$ intermediate as well as intermediates involving σ -bonded ketones, such as $[Cp_2Mo(\sigma-ketone)(H)(D)]^{2+}$.

(40) Zassinovich, G.; Mestroni, G.; Gladiali, S. *Chem. Rev.* **1992**, *92*, 1051–1069.

(41) Noyori, R.; Hashigushi, S. *Acc. Chem. Res.* **1997**, *30*, 97–102.

(42) (a) Aranyos, A.; Csajnyik, G.; Szabó, K.; Bäckvall, J.-E. *Chem. Commun.* **1999**, 351–352. (b) Laxmi, Y. R. S.; Bäckvall, J.-E. *Chem. Commun.* **2000**, 611–612.

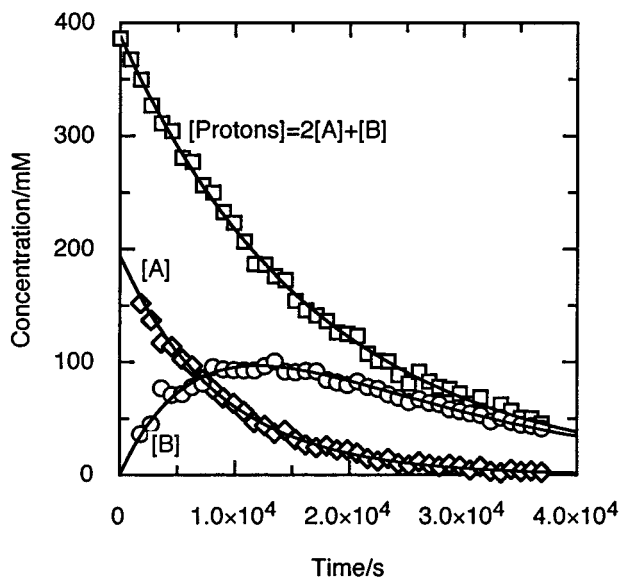
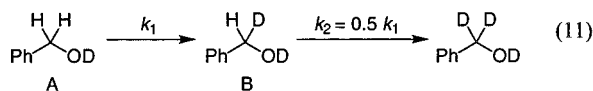


Figure 4. Plot of the concentrations vs time for the deuteration of benzyl alcohol at $T = 90\text{ }^{\circ}\text{C}$.

of **A** and **B** can also be evaluated independently (Figure 4, diamonds and circles, respectively).⁴³

The concentration–time profile depicted in Figure 4 is consistent with a stepwise mechanism (eq 11).



H/D exchange of the first hydrogen is followed by release of the monodeuterated alcohol **B**. Substrate **B** then coordinates again to the metal center and the remaining hydrogen is exchanged. The latter step should occur with only half the frequency of the first exchange because the probability of exchanging the remaining H and thereby leading to a productive reaction (generating PhCD_2OD) is only 50%. Since both steps are chemically identical, the rate constant k_2 for the second step should therefore be equal to $0.5 k_1$.⁴⁴

The integrated rate laws for this stepwise mechanism are shown in eqs 12–14.⁴⁵ $[\text{A}]_0$ represents the initial concentration of benzyl alcohol. The exchange of one hydrogen by deuterium proceeds with a rate constant k_1 .

$$[\text{A}] = [\text{A}]_0 e^{-k_1 t} \quad (12)$$

$$[\text{B}] = 2[\text{A}]_0 e^{-0.5k_1 t} - 2[\text{A}]_0 e^{-k_1 t} \quad (13)$$

$$[\text{protons}] = 2[\text{A}]_0 e^{-0.5k_1 t} \quad (14)$$

Fitting the data⁴⁶ for the decrease in proton concentration, [protons], with eq 14 affords a rate constant of $k_1 = 1.16 \times$

(43) Under some circumstances (unsatisfactory shimming, line broadening as an effect of temperature beyond resolution of the two individual resonances) and at early reaction times (**A** resonances much bigger than and therefore overlapping with **B**), separation of the **A** and **B** resonances is not possible. Rate constants can be obtained, however, from evaluation of the integral over the entire methylene region.

(44) This assumption does not take into account a secondary kinetic isotope effect arising from the nonexchanging C–D bond.

(45) The integrated rate laws (12–14) are based on the following reaction sequence: $\text{A} \xrightarrow{(k_1)} \text{B}$, $\text{B} \xrightarrow{(k_2)} \text{products}$, $k_2 = (1/2)k_1$ with the rate laws $d[\text{A}]/dt = -k_1[\text{A}]$ and $d[\text{B}]/dt = -(k_1/2)[\text{B}] + k_1[\text{A}]$. Evaluating $[\text{A}]$ as $[\text{A}] = [\text{A}]_0 e^{-k_1 t}$ gives the expression $d[\text{B}]/dt = -(k_1/2)[\text{B}] + [\text{A}]_0 e^{-k_1 t}$. With the initial condition $[\text{B}]_0 = 0$, the differential equation is solved to give $[\text{B}] = 2[\text{A}]_0 e^{-0.5k_1 t} - 2[\text{A}]_0 e^{-k_1 t}$. The total concentration of methylene protons is given by $[\text{protons}] = 2[\text{A}] + [\text{B}]$ or $[\text{protons}] = 2[\text{A}]_0 e^{-0.5k_1 t}$.

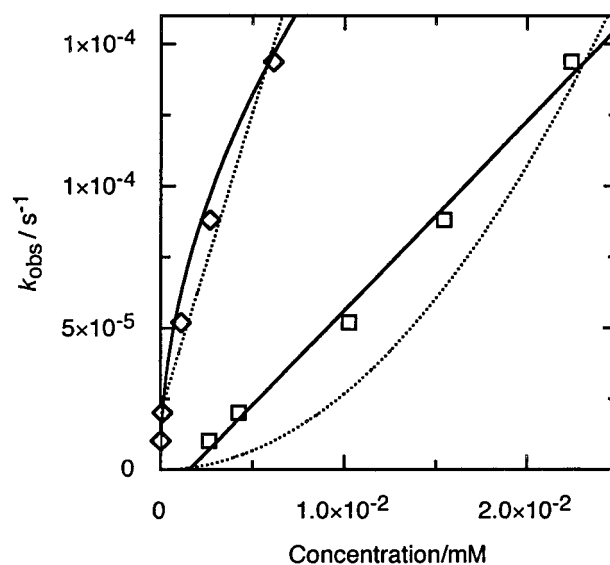


Figure 5. Concentration dependence of k_{obs} at $T = 90\text{ }^{\circ}\text{C}$. Open squares correspond to k_{obs} vs [monomer **2**], open diamonds correspond to [dimer **1**] vs k_{obs} . The solid line shows the fit to the model assuming that k_{obs} is linearly dependent on **[2]**; the dotted line shows the fit to the model considering $k_{\text{obs}} \propto [\text{1}]$.

$10^{-4} (\pm 9.88 \times 10^{-7}) \text{ s}^{-1}$ (Figure 4, solid line through [protons] data). This rate constant was used to calculate concentration profiles for **[A]** and **[B]** (Figure 4, solid lines through **[A]** and **[B]** data), showing good agreement between the kinetic model and the experimental data.

The finding that the H/D exchange occurs stepwise has important mechanistic implications. It means that after incorporation of the first D, the substrate must dissociate from the metal center and then the second D will be incorporated in a second encounter with the catalyst. This implies that the reaction from ketone hydride intermediate **5-d** (Scheme 1) back to aquo hydroxy complex **2**, the reverse of the initial C–H bond activation pathway, is fast, which rules out the possibility that the rate-determining step is in the second half of the cycle, from **5-d** to **2**.

Evidence for a Monomeric Catalyst. Although all of the chemical evidence discussed thus far indicates that the catalytically active species is a monomeric compound (and hence the mechanism is formulated to involve a molybdocene monomer), additional information was sought to unequivocally establish this proposal. For this purpose, H/D exchange was carried out on benzyl alcohol with varying concentrations of catalyst at $T = 90\text{ }^{\circ}\text{C}$. The concentrations of dimer **1** and monomer **2** in the reaction solution were determined from the ^1H NMR spectra. A plot of the observed rate constant, k_{obs} , against **[1]** and **[2]** is shown in Figure 5. Assuming that k_{obs} is proportional to the concentration of monomer **2**, k' , the pseudo-first-order rate constant, is obtained from a linear fit to eq 15 (Figure 5). The dependence of k_{obs} on the concentration of dimer **1** is then given by eq 16. The plot of k_{obs} vs **[1]** with $K_{\text{eq}} = 7.90 \pm 10^{-2} (\pm 1.0 \pm 10^{-3}) \text{ M}^{18}$ is shown in Figure 5.

$$k_{\text{obs}} = k'[\text{2}] \quad (15)$$

(46) Nonlinear data fitting was carried out with the program pro Fit 5.1 using the Levenberg–Marquardt algorithm: QuantumSoft, Postfach 6613, CH-8023, Zürich, Switzerland.

$$k_{\text{obs}} = k' \sqrt{K_{\text{eq}}[\mathbf{1}]}; K_{\text{eq}} = \frac{[\mathbf{2}]^2}{[\mathbf{1}]} \quad (16)$$

Alternatively, k_{obs} could be proportional to the concentration of dimer **1** (eq 17). The corresponding dependence of k_{obs} on monomer **2** is then described by eq 18. The results of linear regression of eq 17 and application of the obtained k' in calculation of the theoretical curve for eq 18 are also shown in Figure 5 (dotted lines).

$$k_{\text{obs}} = k'[\mathbf{1}] \quad (17)$$

$$k_{\text{obs}} = \frac{k'}{K_{\text{eq}}}[\mathbf{2}]^2 \quad (18)$$

From Figure 5 it is apparent that k_{obs} in the H/D exchange reaction is not linearly dependent on **1**. The data, however, are in good agreement with a model assuming a linear dependence of k_{obs} on monomer **2**, from which it is concluded that the active catalyst is a monomeric molybdocene complex.

Kinetic Isotope Effect. The reverse reaction of the H/D exchange, the incorporation of H into a deuterated substrate, was carried out with d_7 -benzyl alcohol (193 mM) and catalyst **1** (15.2 mM) in H_2O . The disappearance of the methylene D resonance was monitored by ^2H NMR at 80 °C, using the resonances of the aromatic deuterium nuclei as reference. The scatter for the NMR data is much larger than in the ^1H NMR experiment, but nevertheless the resulting rates obtained from a fit to eq 14 were reproducible. The average rate constant of three kinetic runs at $T = 80$ °C was $k_{\text{D,pH6.5}} = 2.18 \times 10^{-5}$ ($\pm 2.75 \times 10^{-7}$) s^{-1} . The pH of the reaction solution changed during the course of the reaction, from pH 7.0 prior to heating to pH 6.5 after the kinetic run. The H/D exchange with h_8 -benzyl alcohol (193 mM) in D_2O (15.1 mM in **1**) proceeded with a rate constant of $k_{\text{H,pD7.1}} = 8.13 \times 10^{-5}$ ($\pm 1.07 \times 10^{-6}$) s^{-1} . After completion of the kinetic experiment, the solution had a pD of 7.1. To assess the effect of the slight change in pD on the reaction rate, an H/D exchange experiment was run with benzyl alcohol (193 mM) and **1** (15.2 mM) in D_2O (80 °C), in which the pD was adjusted by adding toluenesulfonic acid, resulting in a reaction solution of pD 6.4.⁴⁷ The reaction rate under these conditions was $k_{\text{H,pD6.4}} = 4.84 \times 10^{-5}$ ($\pm 2.28 \times 10^{-7}$) s^{-1} ,⁴⁸ smaller than $k_{\text{H,pD7.1}}$ yet still considerably higher than $k_{\text{D,pH6.5}}$.

The sensitivity of the H/D reaction to changes in pH does not allow the direct comparison of k_{H} and k_{D} .⁴⁹ However, the ratio $k_{\text{H,pD6.4}}/k_{\text{D,pH6.5}} = 2.2$ is consistent with a primary isotope effect.⁴⁷

In their study on alcohol epimerization (vide supra), Saurallemas and Gladysz³⁷ found $k_{\text{H}}/k_{\text{D}} = 2$ for the epimerization of the alcohol carbon. Similar isotope effects were reported for intramolecular β -hydride elimination reactions of alkyl complexes such as n -octyllithium⁵⁰ and other metal alkyl complexes,⁵¹ with $k_{\text{H}}/k_{\text{D}}$ ranging from 1.5 to 4.7. These examples

(47) Addition of TsOH to the reaction solution resulted in pD 6.4, which is 0.1 unit lower than the pH of the corresponding H_2O solution (it was difficult to adjust the pD to exactly 6.5). Because the H/D reaction slows down with decreasing pH/pD, the calculated primary kinetic isotope effect can be considered a lower limit.

(48) A decrease in pH or pD can contribute to a change in rate if $[\text{H}^+]$ and $[\text{D}^+]$ appear in the rate law. Note that upon decreasing the pD from 7.1 to 6.4, the ^1H NMR spectrum in the Cp' region of **1** and **2** changes significantly, indicating that structural changes occur. These changes in the structure of the active catalyst may also contribute to the decrease in rate.

(49) For an example of $k_{\text{H}}/k_{\text{D}}$ determination without pH correction, see: Jensen, C. M.; Trogler, W. C. *J. Am. Chem. Soc.* **1986**, *108*, 723–729.

(50) Li, M.-Y.; San Filippo, J., Jr. *Organometallics* **1983**, *2*, 554–555.

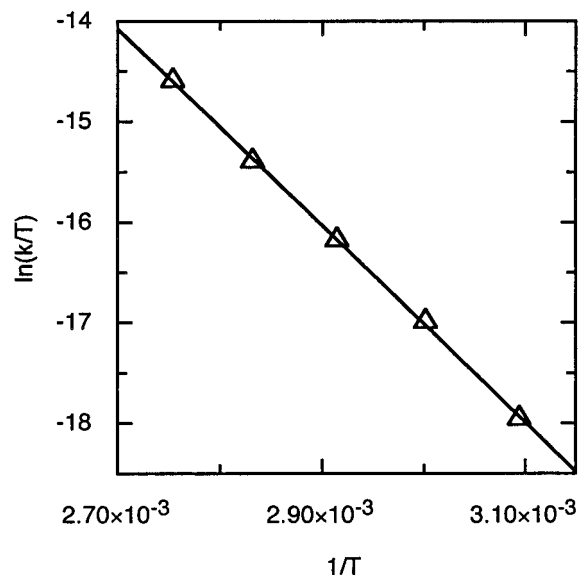


Figure 6. Eyring plot for the deuteration of benzyl alcohol (193 mM) catalyzed by **1** (15.1 mM) in D_2O .

are all consistent with the isotope effect found in this study. The implications of the kinetic isotope effect are discussed below, in conjunction with the activation parameters for the H/D exchange.

Activation Parameters. To obtain information about the activation parameters of the H/D exchange reaction, the deuteration of benzyl alcohol was carried out over the temperature range from 50 to 90 °C in 10 °C intervals. The rates at these temperatures were obtained by fitting the disappearance of the methylene proton resonances of benzyl alcohol to eq 14. An Eyring plot is shown in Figure 6. From a linear regression, the activation parameters were determined as $\Delta H^\ddagger = 19.4$ (± 0.2) kcal mol^{-1} and $\Delta S^\ddagger = -22.7$ (± 0.7) $\text{cal mol}^{-1} \text{K}^{-1}$.⁵²

These activation parameters, particularly the negative activation entropy, indicate that, in the rate-determining step, the transition state acquires a considerable increase in order. This is generally interpreted in terms of an associative process.⁵³ In the first half of the mechanism (Scheme 1), this could apply to the addition of the alcohol to form the alkoxide intermediate, **2** \rightarrow **4**. The addition of alcohol to form **4**, however, does not involve breaking a C–H bond (or any other atom–H bond) and can therefore be ruled out as the rate-determining step. Alternatively, addition of D^+ to the π -ketone intermediate in the course of the H/D exchange (eq 9) would be consistent with a negative activation entropy. This addition reaction, however, involves the breaking of an O–D bond and therefore should occur *more slowly* than the corresponding reaction with a deuterated substrate in H_2O , i.e., a kinetic isotope effect < 1 would be expected. It is therefore unlikely that this latter step in the H/D exchange pathway is rate-determining.

The dissociation of a proton from the ketone intermediate (eq 9) would be consistent with the observed kinetic isotope effect. While this step is dissociative, solvent reorganization could contribute significantly to the activation entropy, resulting

(51) Whitesides, G. M.; Gaasch, J. F.; Stedronsky, E. R. *J. Am. Chem. Soc.* **1972**, *94*, 5258–5270, ref 36.

(52) Activation entropies of similar magnitude have been observed previously in reactions with β -hydrogen-elimination-type rate-determining steps: (a) Van der Boom, M. E.; Higgitt, C. L.; Milstein, D. *Organometallics* **1999**, *18*, 2413–2419 and references therein. (b) Hoffman, D. M.; Lappas, D.; Wierda, D. A. *Organometallics* **1997**, *16*, 972–978. (c) Blum, O.; Milstein, D. *J. Organomet. Chem.* **2000**, *593–594*, 479–484.

(53) Lowry, T. H.; Richardson, K. S. *Mechanism and Theory in Organic Chemistry*, 3rd ed.; Harper Collins Publishers: New York, 1987.

in a negative ΔS^\ddagger . The C–H bond activation step in which the metal center inserts into the carbon–hydrogen bond of the coordinated alkoxide, **4** \rightarrow **5-h**, is also consistent with both the observed activation entropy and the kinetic isotope effect. In this insertion step, the degrees of freedom are reduced significantly in the formation of the ketone hydride complex, giving rise to a negative activation entropy. Furthermore, the α -C–H bond is broken, which is in agreement with the observed isotope effect. Experiments to identify the rate-determining step unambiguously are currently underway.

Summary. The molybdocene-catalyzed H/D exchange reaction is one of the few examples of catalytic C–H bond activation reactions in aqueous solution. Substantial experimental evidence was provided that the mechanism of the catalytic H/D exchange in alcohols promoted by $[\text{Cp}'_2\text{Mo}(\text{OH})(\text{OH}_2)]^+$ (**2**) occurs by the pathway in Scheme 1. Following the exchange of the aquo ligand and coordination of the alcoholic substrate, an alkoxide complex (**4**) is formed. Upon dissociation of the remaining aquo ligand, the coordinatively unsaturated molybdocene inserts into the α -C–H bond of the alkoxide, forming a ketone hydride intermediate (**5-h**). The ketone is labile toward dissociation, which opens up the possibility of using the molybdocene catalyst in hydrogen transfer reactions, whether it is in oxidations of alcohols using a sacrificial ketone as a reducing agent or the reduction of a ketone employing a sacrificial alcohol. Ketone hydride complex **5** can undergo reversible protonation, which leads to the observed isotope exchange upon dissociation of the coordinated alcohol.

Experimental Section

All manipulations were carried out in a nitrogen atmosphere using standard vacuum line techniques or a glovebox. Solvents were dried over and distilled from the appropriate drying agents.⁵⁴ All alcohols were dried over and distilled from CaH_2 . *d*₇-Benzyl alcohol (97% D) was purchased from Aldrich and used as received. D₂O (99.9% D) was purchased from Cambridge Isotope Laboratories and purged with N₂ for at least 30 min prior to use. ¹H and ²H NMR spectra were recorded using a Varian Inova 300 (299.95 MHz for ¹H, 46.04 MHz for ²H) or a GE 500 (500.13 MHz for ¹H, 76.77 MHz for ²H) spectrometer. $[\text{Cp}'_2\text{Mo}(\mu\text{-OH})_2\text{MoCp}'_2](\text{OTs})_2$ ¹⁹ and $\text{Cp}'_2\text{MoH}_2$ ⁵⁵ were prepared according to literature procedures. NMR samples were prepared in the glovebox. NMR experiments at higher temperatures were carried out in 5 mm NMR tubes which were flame-sealed while frozen in N₂(*l*) prior to heating. pH measurements on NMR samples were carried out using a Corning NMR Micro Electrode, *d* = 3 mm, and a Hanna HI9023 pH meter with attached thermocouple. Prior to the measurement, the NMR tube was placed in a water bath together with the thermocouple to allow for thermal equilibration. All reported pD values were calculated according to pD = (pH meter reading + 0.4) to correct for the use of a glass electrode.^{56,57} Elemental analyses were carried out by Robertson Microлит Laboratories, Inc., Madison, NJ.

Synthesis of $[\text{Cp}'_2\text{MoOCH}_2\text{CH}_2\text{OH}][\text{OTs}]$ (6**).** To a solution of 133 mg (0.15 mmol) of $[\text{Cp}'_2\text{Mo}(\mu\text{-OH})_2\text{MoCp}'_2](\text{OTs})_2$ in 10 mL of MeOH was added 60 μL of ethylene glycol (67 mg, 1.08 mmol), and the reaction mixture was refluxed for 16 h. The solvent was removed in vacuo to give an orange oil. Trituration of the oil with THF afforded an orange solid. Orange crystals were grown by layering Et₂O onto a solution of **6** in MeOH/THF (1:1) and cooling to -30°C . ¹H NMR (300 MHz, D₂O): δ 7.48 (d, 6.5 Hz, OTs, 2H), 7.36 (d, 7.8 Hz, OTs, 2H), 5.38 (m, 4H), 5.33 (m, 4H), 3.24 (s, 4H), 2.37 (s, OTs–CH₃, 3H), 1.83 (s, 6H). Anal. Calcd for C₂₁H₂₆MoO₅S: C, 51.85; H, 5.39;

(54) Perrin, D. D.; Armarego, W. L. F. *Purification of Laboratory Chemicals*, 3rd ed.; Pergamon Press: Oxford, 1988.

(55) Luo, L.; Lanza, G.; Fraga, I. L.; Stern, C. L.; Marks, T. J. *J. Am. Chem. Soc.* **1998**, *120*, 3111–3122.

(56) Glasoe, P. K.; Long, F. A. *J. Phys. Chem.* **1960**, *64*, 188–190.

(57) Mikkelsen, K.; Nielsen, S. O. *J. Phys. Chem.* **1960**, *64*, 632–637.

Table 2. Crystallographic Data for **6**

composition	C ₂₁ H ₂₆ MoO ₅ S
formula wt	486.43
crystal system	triclinic
space group	P(–1)
<i>a</i>	12.233(2) Å
<i>b</i>	12.779(3) Å
<i>c</i>	14.825(2) Å
α	89.40(2)°
β	73.53(2)°
γ	68.79(2)°
<i>V</i>	2061(1) Å ³
<i>Z</i>	4
<i>d</i> _{calc}	1.568 g cm ^{–3}
<i>T</i>	22 °C
radiation, λ	Mo K α , 0.71073 Å
μ	7.66 cm ^{–1}
no. obs. rflns	3344 [<i>I</i> \leq $\sigma(I)$]
no. indep. rflns	4472
<i>R</i> (<i>F</i>), ^a w <i>R</i> (<i>F</i>) (obs.)	0.067, 0.087
<i>R</i> (<i>F</i> ²), w <i>R</i> (<i>F</i> ²) (all)	0.042, 0.043

$$^a R(F) = \frac{\sum ||F_o| - |F_c||}{\sum |F_o|}; \text{w}R(F^2) = \frac{[\sum w(|F_o|^2 - |F_c|^2)^2]}{\sum w|F_o|^4}]^{1/2}.$$

Mo, 19.72. Found: C, 51.55; H 5.19; Mo, 19.04. The complex converts rapidly to **2** and free ethylene glycol when dissolved in D₂O.

X-ray Structure Analysis of $[\text{Cp}'_2\text{MoOCH}_2\text{CH}_2\text{OH}][\text{OTs}]$ (6**).** A crystal of dimensions 0.04 \times 0.17 \times 0.32 mm was mounted on a fiber with a coating of epoxy. The orientation parameters and cell dimensions were obtained from the setting angles of an Enraf-Nonius CAD-4 diffractometer for 25 centered reflections in the range $12.0^\circ \leq \theta \leq 13.9^\circ$. Table 2 contains a summary of crystal data and the final residuals. A more extensive table including particulars of data collection and structure refinement can be found in the Supporting Information. The crystal decayed progressively and data collection was halted near the end of the shell $17^\circ \leq \theta \leq 22^\circ$, when the intensities of standard reflections had decreased 20%. The centric distribution of intensities indicated the space group *P*(–1). A SIR92 *E*-map⁵⁸ showed all non-hydrogen atoms of the two independent formula units. Empirical absorption corrections based on the isotropically refined structure (DIFABS⁵⁹) resulted in no significant decrease in the residuals and standard deviations, and the results presented here are for uncorrected data. Hydrogen atoms bonded to carbon were included at positions recalculated after each cycle of refinement [*B*(H) = 1.2*B*_{eq}(C); *d*(C–H) = 0.95 Å]. The final difference map confirmed that the compound was unsolvated. The teXsan program suite,⁶⁰ incorporating complex atomic scattering factors, was used in all calculations.

Synthesis of $\text{Cp}'_2\text{MoH}(\text{OTf})$ (8**).** In the glovebox, a solution of 100 mg (0.39 mmol) of $\text{Cp}'_2\text{MoH}_2$ in 5 mL of benzene was prepared. 45 mL (65 mg, 0.40 mmol) of MeOTf was added, and the solution was stirred for 1 h. A reddish solid formed instantly, and evolution of gas bubbles was observed. The solvent was decanted off, and the precipitate was washed with hexanes. The solid was recrystallized from hot benzene. ¹H NMR (300 MHz, C₆D₆): δ 4.87 (m, 2H), 4.66 (m, 2H), 4.08 (m, 2H), 3.57 (m, 2H), 1.59 (s, 6H, Me), –8.41 (s, 1H) ¹H NMR (300 MHz, D₂O): δ 5.60 (m, 2H), 5.47 (m, 2H), 4.62 (m, 2H), 4.56 (m, 2H), –9.26 (m, 1H). Anal. Calcd for C₁₃H₁₅F₃MoO₃S: C, 38.62; H, 3.74. Found: C, 38.77; H 3.52.

X-ray Structure Analysis of $\text{Cp}'_2\text{MoH}(\text{OTf})$ (8**).** A dark red block of dimensions 0.29 \times 0.36 \times 0.49 mm was sealed in a special glass capillary in the drybox. The orientation parameters and cell dimensions were obtained from the setting angles of an Enraf-Nonius CAD-4 diffractometer for 25 centered reflections in the range $13.8^\circ \leq \theta \leq 14.9^\circ$. Table 3 contains a summary of crystal data and the final residuals. A more extensive table including particulars of data collection and structure refinement can be found in the Supporting Information. The

(58) Altomare, A.; Cascarano, G.; Giacovazzo, C.; Guagliardi, A.; Burla, M. C.; Polidori, G.; Camalli, N. *J. Appl. Crystallogr.* **1994**, *27*, 435.

(59) Walker, N.; Stuart, D. *Acta Crystallogr.*, A **1983**, *39*, 158–166.

(60) Molecular Structures Corporation, 3200A Research Forest Drive, The Woodlands, TX 77381. teXsan Software for Single-Crystal Structure Analysis, version 1.7, 1997.

Table 3. Crystallographic Data for **8**

composition	C ₁₃ H ₁₅ F ₃ MoO ₃ S
formula wt	404.25
crystal system	orthorhombic
space group	<i>Pbcm</i>
<i>a</i>	12.0180(14) Å
<i>b</i>	8.6571(6) Å
<i>c</i>	13.9728(22) Å
<i>V</i>	1453.7(3) Å ³
<i>Z</i>	4
<i>d</i> _{calc}	1.847 g cm ⁻³
<i>T</i>	22 °C
radiation, λ	Mo Kα, 0.71073 Å
μ	10.8 cm ⁻¹
rel. trans. coeff.	0.863–1.000 (<i>φ</i>)
no. obs. rflns	2251 [<i>I</i> ≥ <i>σ</i> (<i>I</i>)]
no. indep. rflns	2983 (265 syst. abs.)
<i>R</i> (<i>F</i>), ^a w <i>R</i> (<i>F</i>)	0.029, 0.033

$$^a R(F) = \sum ||F_o| - |F_c|| / \sum |F_o|; wR(F) = [\sum w(|F_o| - |F_c|)^2 / \sum w|F_o|^2]^{1/2}.$$

systematic absences together with the centric distribution of intensities indicated the space-group *Pbcm*. A SIR92 *E*-map⁵⁸ showed all non-hydrogen atoms of the half-molecule constituting the asymmetric unit. An *E*-map in the alternative space group *Pbc2*₁ gave the same molecule, with a clear mirror-plane normal to *c*. Absorption corrections based on azimuthal scans (“*ψ* scans”) were applied. All hydrogen atoms were located and refined isotropically. The teXsan program suite,⁶⁰ incorporating complex atomic scattering factors, was used in all calculations.

Deuteration of Alcoholic Substrates. In the glovebox, 7–15 mg (7.9–17.0 μmol) of **1** was dissolved in 0.7–1.4 mL of D₂O. To the green-brown solution 30–40 μL of alcohol was added. The resulting solutions were transferred to NMR tubes which were subsequently sealed. Initial ¹H and ²H NMR spectra were recorded, and the samples were placed in a temperature-controlled oil bath. The reaction progress was monitored regularly by ¹H and ²H NMR.

Transfer Hydrogenation. In the glovebox, 16 mg (18 μmol) of **1**, 30 μL (355 μmol) of 2-butanone, and 27 μL (352 μmol) of 2-propanol were dissolved in 1 mL of D₂O. The solution was transferred to two NMR tubes which were subsequently sealed. Initial ¹H and ²H NMR spectra were recorded, and the samples were placed in a temperature-controlled oil bath at 80 °C. The reaction progress was monitored regularly by ¹H and ²H NMR.

Stepwise Exchange. In the glovebox, a solution of 54.9 mg (62 μmol) of **1**, 100 μL (996 μmol) of benzyl alcohol, and D₂O was prepared in a 5 mL volumetric flask. The solution was stirred until all of the solid had dissolved. The solution was transferred to NMR tubes which were subsequently sealed. One sample at a time was placed in the NMR magnet, and the VT temperature was controlled at 60, 70, 80, and 90 °C, respectively. ¹H NMR spectra were recorded in 20 min intervals with 4 scans/spectrum. The entire methylene proton resonance, consisting of contributions from C₆H₅CH₂OD (**A**) and C₆H₅CHDOD (**B**), was integrated versus the resonance corresponding to the aromatic protons. In addition, the individual contributions of **A** and **B** were evaluated by integration of their respective resonances versus the resonance corresponding to the aromatic protons.

Catalyst-Concentration Dependence. In the glovebox, a solution of 76.7 mg (86.7 μmol) of **1**, 500 μL (4.83 mmol) of benzyl alcohol,

and D₂O was prepared in a 25 mL volumetric flask. The solution was stirred until all solid had dissolved. This solution was successively diluted by a factor of 3/5, adding 2 mL of reaction solution and D₂O to a 5 mL volumetric flask. Samples with catalyst concentrations of 17.3, 10.4, 6.24, 2.25, and 1.35 mM were transferred to NMR tubes which were subsequently sealed. Concentrations of **1** and **2** after hydrolysis were obtained by integrating the CpCH₃ resonances in the ¹H NMR spectrum at δ = 1.81 and 1.93 ppm, respectively, versus the integral of the ⁻O₃SC₆H₄CH₃ resonance at δ = 2.40 ppm. The VT temperature was controlled at 90 °C, and ¹H NMR spectra were recorded in 20 min intervals with 4 scans/spectrum.

Temperature Dependence. In the glovebox, a solution of 133.9 mg (151 μmol) of **1**, 200 μL of benzyl alcohol (1.93 mmol), and D₂O was prepared in a 10 mL volumetric flask. The reaction solution was transferred to several NMR tubes which were subsequently sealed. For the kinetic measurements, the VT temperature of the NMR was controlled at 50, 60, 70, 80, and 90 °C, and spectra were collected at intervals of 60, 30, or 15 min, respectively. The concentration of methylene protons was evaluated by comparing their integral to the integral corresponding to the aromatic protons. Rate constants were obtained by fitting the [protons] vs time data to eq 14.

D/H Exchange in *d*₇-Benzyl Alcohol. In the glovebox, a solution of 133.7 mg (151 μmol) of **1**, 200 μL of *d*₇-benzyl alcohol (1.93 mmol), and H₂O was prepared in a 10 mL volumetric flask. The reaction solution was transferred to several NMR tubes which were subsequently sealed. For the kinetic measurements, the VT temperature of the NMR was controlled at 80 °C and spectra were collected in 30 min intervals, using the lock channel of a 5 mm broadband probe of a GE 500 spectrometer to detect the ²H signal. The concentration of methylene protons was evaluated by comparing their integral to the integral corresponding to the aromatic protons. Rate constants were obtained by fitting the [protons] vs time data to eq 14. ¹H NMR spectra of the reaction solution before the kinetic runs were acquired on a Varian Inova 300 spectrometer using the presat water suppression pulse sequence supplied with the Varian VNMR 6.1 software.

H/D Exchange at pD 6.4. To a solution of benzyl alcohol (193 mM) and **1** (15.2 mM) in D₂O was added toluenesulfonic acid monohydrate to afford a solution of pD 6.4. Kinetic experiments were carried out as described above. As determined after the kinetic runs, the solution had maintained pD 6.4.

Acknowledgment. This research was supported by the National Science Foundation. We thank Dr. Michael Strain for his assistance with the NMR experiments and Professors Louis Y. Kuo (Lewis and Clark College) and Kevin P. Gable (Oregon State University) for useful discussions.

Supporting Information Available: A scheme illustrating the equilibria between **2**, **4**, and **5**, with qualitative estimations of rates. Additional crystallographic information including particulars of data collection and structure refinement for **6** and **8**. This material is available free of charge via the Internet at <http://pubs.acs.org>.

JA001535V